Arabian Journal of Chemistry (2014) xxx, xxx–xxx

King Saud University

Arabian Journal of Chemistry

www.ksu.edu.sa
www.sciencedirect.com

ORIGINAL ARTICLE

Electrochemical measurements for the corrosion inhibition of mild steel in 1 M hydrochloric acid by using an aromatic hydrazide derivative

P. Preethi Kumari [a], Prakash Shetty [b,*], Suma A. Rao [a]

[a] Department of Chemistry, Manipal Institute of Technology, Manipal University, Manipal 576104, India
[b] Department of Printing and Media Engineering, Manipal Institute of Technology, Manipal University, Manipal 576104, India

Received 19 September 2013; accepted 6 September 2014

KEYWORDS

Mild steel;
Tafel polarization;
Acid corrosion;
EIS;
SEM

Abstract The influence of an aromatic hydrazide derivative, 2-(3,4,5-trimethoxybenzylidene) hydrazinecarbothioamide (TMBHC) as corrosion inhibitor on mild steel in 1 M hydrochloric acid was studied by Tafel polarization and electrochemical impedance spectroscopy (EIS) technique. The results showed that the inhibition efficiency (% *IE*) of TMBHC increased with increasing inhibitor concentrations and also with increase in temperatures. TMBHC acted as a mixed type of inhibitor and its adsorption on mild steel surface was found to follow Langmuir's adsorption isotherm. The evaluation of thermodynamic and activation parameters indicated that the adsorption of TMBHC takes place through chemisorption. The formation of protective film was further confirmed by scanning electron microscopy (SEM).

1. Introduction

Mild steel is an important material which finds wide applications in industry due to its excellent mechanical properties and low cost. It is extensively used in various industries as construction material for chemical reactors, heat exchanger and boiler systems, storage tanks, and oil and gas transport pipelines (Tao et al., 2009; Singh and Quraishi, 2012). It is also used in chemical and allied industries in handling acids, alkalis and salt solutions.

Acid solutions are widely used in industry for processes such as acid pickling of iron and steel, chemical cleaning and oil well acidification. Hydrochloric acid is widely used as it is more economical and trouble free than other mineral acids (Singh et al., 1995). The main advantage of this acid over other acids in cleaning and pickling operations lies in its ability to form metal chloride, which is extremely soluble in aqueous medium, compared to sulphate phosphate and nitrate. The higher solubility of chloride salt causes the least polarizing effect and does not hinder the rate of corrosion (Hudson and Warning, 1970; Emregul and Hayval, 2006). The use of corrosion inhibitors is considered the most effective method for the protection of many metals and alloys against such acid attack.

* Corresponding author. Tel.: +91 820 2925661; fax: +91 820 2571071.
E-mail address: prakash.shetty@manipal.edu (P. Shetty).

Peer review under responsibility of King Saud University.

ELSEVIER Production and hosting by Elsevier

http://dx.doi.org/10.1016/j.arabjc.2014.09.005

Hence the study of corrosion on mild steel in acid media is of both academic and industrial concern and has received a considerable amount of attention of many investigators.

Most of the acid corrosion inhibitors are organic compounds containing electronegative atoms (such as O, N, S, and P etc.), unsaturated bonds and/or aromatic rings (Bentiss et al., 2001; Hosseini et al., 2003; Singh, 2012). The compounds having the –C═N– group, electron donating groups, polar groups, and π electrons are reported to behave as effective inhibitors of mild steel in acid medium (Fekry and Riham, 2010; Nada et al., 2011; Hegazy et al., 2011). Even though many aromatic hydrazide derivatives were studied as corrosion inhibitors of mild steel, most of them failed to show good inhibition efficiency at higher temperatures (Quraishi et al., 2001; Shanbhag et al., 2008; Badr, 2009).

The aim of the present work is to study the influence of 2-(3,4,5-trimethoxybenzylidene) hydrzinecarbothiamide (TMBHC), as a corrosion inhibitor for mild steel in 1 M hydrochloric acid using Tafel polarization and EIS methods. Further the study also focuses on the inhibition mechanism based on the adsorption isotherms, activation and thermodynamic parameters obtained.

2. Experimental

2.1. Synthesis of TMBHC

2-(3,4,5-trimethoxybenzylidene) hydrazinecarbothioamide (TMBHC) was synthesized as per the reported literature (Renata et al., 2008). An equimolar mixture of ethanolic solution of 3,4,5-tri methoxy benzaldehyde and thiosemicarbazide was refluxed on a hot water bath for about 2 h. The precipitated product obtained, was purified by recrystallization using ethanol and characterized by spectral techniques like infrared spectroscopy (Schinadzu FTIR 8400S Spectrophotometer) and NMR spectroscopy (Bruker Avalanche-400 MHz). The purity of the compound was checked by CHN analysis. Fig. 1 represents the structure of TMBHC.

2.2. Medium

The standard solution of 1 M hydrochloric acid was prepared using an AR grade sample and double distilled water. The experiments were performed in 1 M HCl in the absence and presence of TMBHC (0.1–0.8 mM), at different temperatures (30–60 °C).

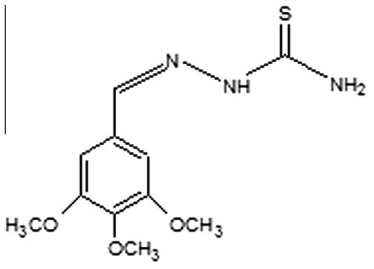

Figure 1 Structure of the TMBHC molecule.

2.3. Material

Mild steel specimen with composition of (% wt) C (0.159), Si (0.157), Mn (0.496), P (0.060), S (0.062), Cr (0.047), Ni (0.06), Mo (0.029), Al (0.0043), Cu (0.116) and remaining Fe was used in the present work. The specimens were taken in the form of a cylindrical rod of 5 cm height, embedded in epoxy resin, by leaving one end of the rod with an open surface area of 0.95 cm^2. They were abraded using emery papers of different grades and subsequently on disc polished using levigated alumina. The abraded specimen was cleaned with double distilled water followed with acetone, and finally dried.

2.4. Electrochemical measurements

Electrochemical measurements such as Tafel polarization and electrochemical impedance were carried out using an electrochemical work station (CH Instrument USA Model 604D series with beta software). The electrochemical cell consists of conventional three-electrode Pyrex glass cell with platinum as counter electrode, saturated calomel electrode (SCE) as reference electrode and mild steel specimen as working electrode.

The freshly polished mild steel specimen was exposed to corrosive medium of 1 M hydrochloric acid in the absence as well as the presence of TMBHC at different temperatures. The steady-state open circuit potential (OCP) was allowed to establish. The impedance experiments were carried out in the frequency range of 100 kHz–0.01 Hz, at the OCP by applying small amplitude ac signal of 10 mV. Tafel plots (current vs. potential) were recorded soon after the impedance measurement by polarizing the specimen from −250 mV cathodically to +250 mV anodically with respect to OCP at a scan rate of 1 mV s^{-1}.

2.5. Scanning electron microscopy (SEM)

The surface morphology of the mild steel specimen immersed in 1 M hydrochloric acid in the absence and presence of TMBHC was recorded by using a Scanning electron microscopy (EVO 18-5-57 model).

3. Results and discussion

3.1. Characterization of TMBHC

Yield 95%, yellow solid, m.p. 262–268 °C., IR (KBr, ν_{max} cm^{-1}; 3556, 3394 (NH_2 str.), 3263 (NH str.), 3163 (Ar. C–H str.), 2939 (CH_3 asym str.), 2823 (CH_3 sym str.), 1620 (C═N), 1573 (Ar. C═C str), 1234 (C═S); ^{1}H NMR (400 MHz, $CDCl_3$) δ (ppm): 11.43 (1H, NH), 8.24 (1H, CH═N), 7.95–8.10 (2H, Ar. H), 7.09 (2H, NH_2) 3.83 (6H, OCH_3), 3.68 (3H, OCH_3); Anal. Calcd. for $C_{11}H_{15}N_3O_3S$: C, 49.07; H, 5.58; N, 15.61. Found: C, 49.17; H, 5.61; N, 15.63. Figs. 2 and 3 represent the IR and NMR spectrum of the TMBHC molecule.

3.2. Tafel polarization measurements

The polarization studies of mild steel specimens were carried out in 1 M hydrochloric acid solution both in the absence

Please cite this article in press as: Preethi Kumari, P. et al., Electrochemical measurements for the corrosion inhibition of mild steel in 1 M hydrochloric acid by using an aromatic hydrazide derivative. Arabian Journal of Chemistry (2014), http://dx.doi.org/10.1016/j.arabjc.2014.09.005

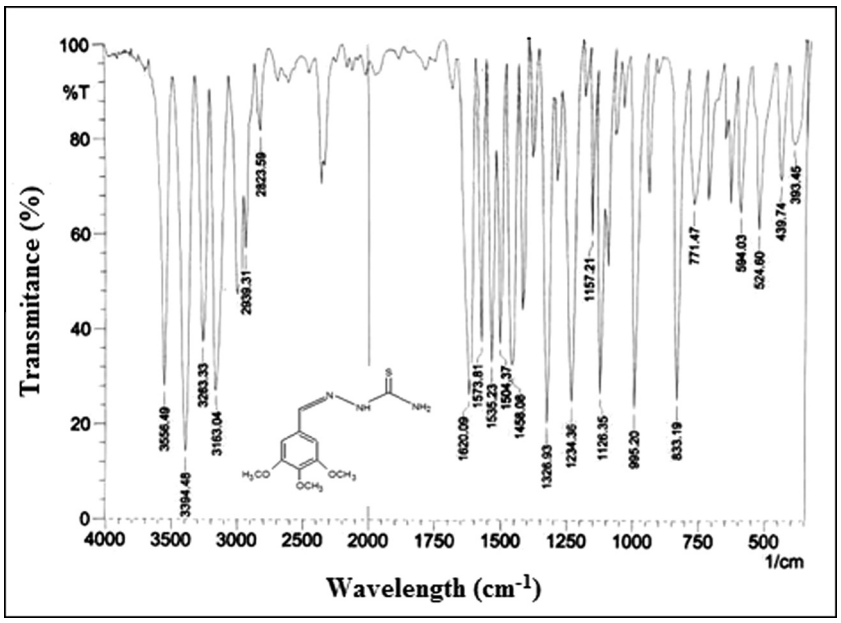

Figure 2 IR spectrum of the TMBHC molecule.

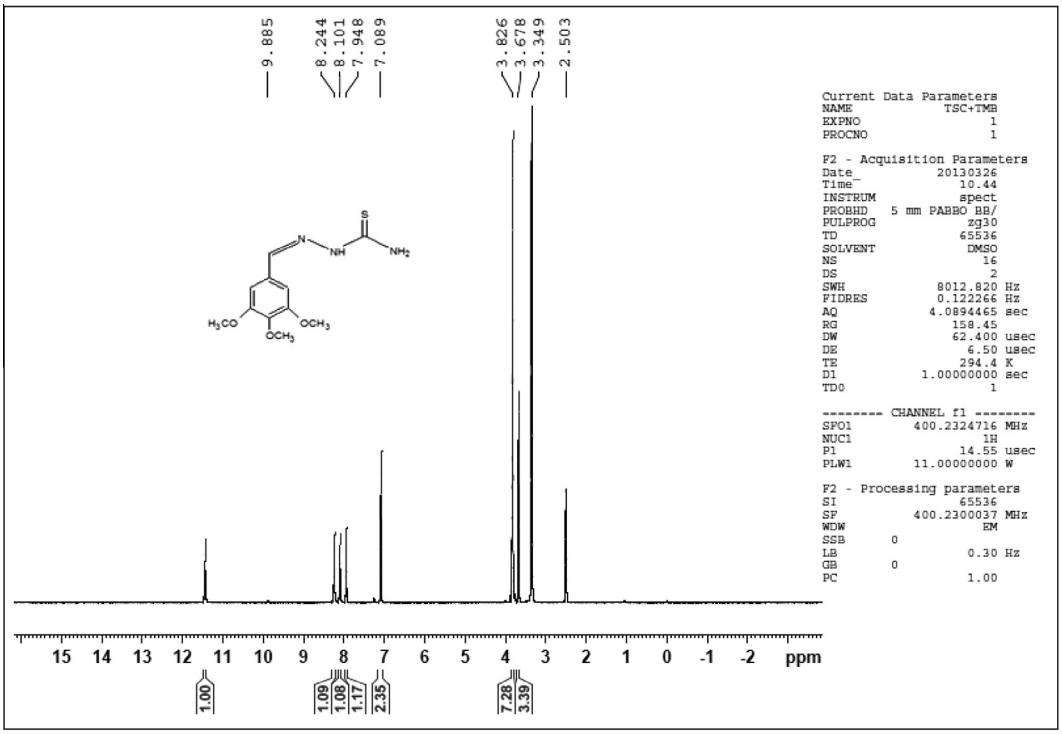

Figure 3 NMR spectrum of the TMBHC molecule.

and presence of different concentrations of TMBHC. Fig. 4 shows the Tafel polarization curves for the dissolution of mild steel in 1 M hydrochloric acid solution at 40 °C in the absence and presence of TMBHC. The Tafel parameters such as corrosion potential (E_{corr}), corrosion current density (i_{corr}), corrosion rate (CR), cathodic slope (b_c) and percentage efficiency (% IE) are computed and tabulated in Table 1.

The corrosion rate (CR) is calculated using Eq. (1).

$$CR\ (\text{mmpy}) = \frac{3270 \times M \times i_{corr}}{\rho \times Z} \quad (1)$$

where the constant, 3270 represents the unit of corrosion rate, i_{corr} = corrosion current density in A cm^{-2}, ρ = density of the corroding material (7.74 g cm^{-3}), M = Atomic mass of the metal (55.85), and Z = Number of electrons transferred per metal atom (Z = 2).

Please cite this article in press as: Preethi Kumari, P. et al., Electrochemical measurements for the corrosion inhibition of mild steel in 1 M hydrochloric acid by using an aromatic hydrazide derivative. Arabian Journal of Chemistry (2014), http://dx.doi.org/10.1016/j.arabjc.2014.09.005

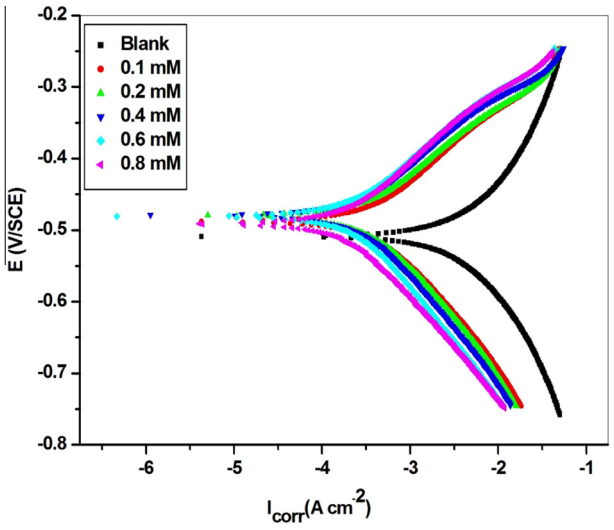

Figure 4 Tafel polarization curves for mild steel immersed in 1 M HCl with various concentrations of TMBHC at 40 °C.

The surface coverage (θ) on the metal surface and the percentage inhibition efficiency (% *IE*) are calculated using Eqs. (2) and (3), respectively (Shahin et al., 2003).

$$\theta = \frac{i_{corr} - i_{corr(inh)}}{i_{corr}} \quad (2)$$

where i_{corr} and $i_{corr(inh)}$ represent the corrosion current densities in the presence of uninhibited and inhibited solutions, respectively.

$$\%\ IE = \theta \times 100 \quad (3)$$

The value of *CR* of mild steel in the absence of TMBHC increased with rise in temperature. The addition of inhibitor brought down the corrosion current as well as the corrosion rate to the controlled level. Further the inhibition efficiency increased with increase in TMBHC concentrations and also with increase in temperature. The maximum efficiency in the range 90–95% is attained at an optimum concentration (0.8 mM) of TMBHC.

It is evident from Table 1 that the addition of TMBHC shows a positive shift in the E_{corr} value. It is reported (Li et al., 2008) that if the shift in corrosion potential exceeds ±85 mV with respect to corrosion potential of the uninhibited solution, the inhibitor acts as either anodic or cathodic type. In the present case the maximum displacement in E_{corr} is found to be within +20 mV, which indicates that TMBHC acts as mixed type of inhibitor by showing its inhibitory action on both hydrogen evolution and metal dissolution (Li et al., 2007). Further it is observed from Fig. 4 that the anodic polarization curves did not exhibit linear behaviour and are assumed to represent anodic oxidation of steel. The anodic branches showed the inflection points at potentials more positive than corrosion potential (E_{corr}), characterized by two different slopes indicating a kinetic barrier effect, possibly due to the deposition of a surface film followed by its dissolution at increased anodic potential (Zhao et al., 2008). However the cathodic polarization curves showed linear behaviour and values of cathodic slope (b_c) did not vary significantly with increase in inhibitor concentration, which indicates that the hydrogen evolution is activation-controlled and the presence of inhibitor does not alter the inhibition mechanism (El Kadher et al., 1998).

Table 1 Tafel polarization parameters for the corrosion of mild steel in 1 M HCl in the absence and presence of various concentrations of TMBHC.

Temp. (°C)	Conc. of inhibitor (mM)	E_{corr} (V/SCE)	$-b_c$ (mV dec^{-1})	i_{corr} (mA cm^{-2})	*CR* (mpy)	% *IE*
30	0	−507	73.14	1.894	462.3	–
	0.1	−490	61.72	0.359	87.71	81.0
	0.2	−491	51.14	0.301	73.50	84.1
	0.4	−492	53.08	0.271	66.22	85.6
	0.6	−492	56.75	0.241	58.99	87.2
	0.8	−494	58.23	0.192	46.99	89.8
40	0	−505	68.71	3.352	818.0	–
	0.1	−495	75.83	0.413	100.8	87.4
	0.2	−496	76.62	0.338	82.69	89.7
	0.4	−495	73.65	0.275	65.36	91.6
	0.6	−495	79.39	0.246	60.22	92.5
	0.8	−498	78.97	0.213	52.17	93.5
50	0	−504	61.32	6.458	1576	–
	0.1	−500	78.07	0.696	170.1	88.1
	0.2	−504	70.29	0.506	123.5	91.3
	0.4	−503	70.48	0.428	104.5	92.6
	0.6	−502	70.38	0.377	92.05	93.4
	0.8	−508	71.25	0.338	82.66	94.2
60	0	−504	54.28	12.43	3032	–
	0.1	−498	71.74	1.301	317.6	88.5
	0.2	−508	71.85	0.843	205.8	92.5
	0.4	−517	72.32	0.694	169.4	93.8
	0.6	−508	74.81	0.648	158.3	94.2
	0.8	−508	75.75	0.583	142.2	94.8

Please cite this article in press as: Preethi Kumari, P. et al., Electrochemical measurements for the corrosion inhibition of mild steel in 1 M hydrochloric acid by using an aromatic hydrazide derivative. Arabian Journal of Chemistry (2014), http://dx.doi.org/10.1016/j.arabjc.2014.09.005

3.3. Electrochemical impedance spectroscopy

The effect of inhibitor concentration on the impedance behaviour of mild steel in 1 M hydrochloric acid is studied and the corresponding results are compared with the results of Tafel polarization experiments. The Nyquist plots recorded for the corrosion inhibition of mild steel with different concentrations of TMBHC at 40 °C in 1 M hydrochloric acid are shown in Fig. 5. The Nyquist plots were obtained with depressed semicircle in the presence of inhibitor. It is also observed that the diameter of the impedance plot increased with increase in inhibitor concentration. The depression in the semicircles is often attributed to the surface roughness, inhomogeneity of the solid surface and adsorption of the inhibitor on the metal surface (Amin et al., 2007; Wei-hua et al., 2008).

Suitable equivalent circuits are used to analyse the impedance data, depending upon the shapes of the Nyquist plots. A simplest Randles equivalent circuit as shown in Fig. 6(a) is used to fit the Nyquist plot in the absence of inhibitor in 1 M hydrochloric acid solution. It consists of solution resistance R_s, charge transfer resistance R_{ct} and one constant phase element (CPE). CPE was employed instead of the double-layer capacitance (C_{dl}) to describe the heterogeneity in the system. The Nyquist plots for the corrosion inhibition of mild steel in the presence of inhibitor consisted of one distorted capacitive loop at higher frequency due to charge transfer reaction and the time constant of the electric double layer (Singh and Quraishi, 2010). Suitable equivalent circuit is used to simulate the impedance data in the presence of TMBHC as shown in Fig. 6(b). Similar circuits were used to model steel acid interface in the presence of inhibitor (Lowmunkhong et al., 2010). It included the solution resistance (R_s), fast charge transfer process (R_1), time constant of the electric double layer (CPE_1), the capacitance of the surface film (CPE_2) and the surface layer resistance (R_2). Both R_1 and R_2 increased with increase in inhibitor concentration at all studied temperatures. The impedance parameters obtained are reported in Table 2.

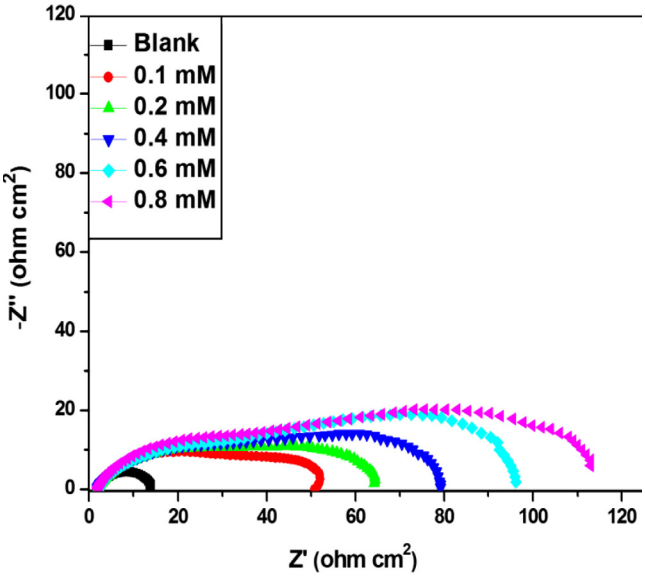

Figure 5 Nyquist plots for the mild steel specimen in 1 M HCl acid containing different concentrations of TMBHC at 40 °C.

The CPE impedance is calculated using the Eq. (4) (Raistrick et al., 2005).

$$Z = A^{-1}(iw)^{-n} \tag{4}$$

where A is the proportionality coefficient, w is the angular frequency, i is the imaginary number and n is the exponent related to the phase shift. If the value of $n = 1$, the CPE behaves like an ideal capacitor. The correction in the capacitance to its real value is calculated using the relation (5) (Machnikova et al., 2008).

$$C_{dl} = \frac{1}{2\pi f_{max} R_{ct}} \tag{5}$$

where, $f_{\max}$ is the frequency at which the imaginary component of impedance is maximum and R_{ct} is the charge transfer resistance.

The measured C_{dl} value decreased with increase in inhibitor concentration at all studied temperatures. The decrease in C_{dl} value can be attributed to the increase in the electrical double layer at the metal solution interface. This suggests that the inhibitor acts via adsorption at the metal/solution interface. Further the decrease in the C_{dl} values is caused by the gradual replacement of water molecules by the adsorption of the inhibitor molecules on the electrode surface, which decreases the extent of metal dissolution (Legrenee et al., 2002).

The polarization resistance R_p, which is equivalent to charge transfer resistance R_{ct} is calculated by the summation of R_1 and R_2 at different concentrations of inhibitor and the resultant R_{ct} is used to calculate the percentage inhibition efficiency using Eq. (6) (Wang et al., 2010).

$$\%\ IE = \frac{R_{ct} - R^{\circ}_{ct}}{R_{ct}} \times 100 \tag{6}$$

where, R_{ct} and R°_{ct} indicate the charge transfer resistances in the presence and absence of TMBHC, respectively. The values of R_{ct} increased with rise in the inhibitor concentration, and the results indicated that the charge transfer process is mainly controlling the corrosion process.

Bode plot for the corrosion of mild steel in the presence of different concentrations of TMBHC at 40 °C is shown in Fig. 7. It is observed from the plot that the phase angle increases with increase in the concentration of TMBHC up to an optimal level. The difference between the high frequency (HF) limit and low frequency (LF) limit in the Bode plot is equal to polarization resistance (R_p). The polarization resistance is associated with the dissolution and repassivation processes occurring at the interface as well as the electronic conductivity of the film. The difference between the HF and LF for the uninhibited and inhibited systems in the Bode plot increases with increase in the inhibitor concentration of TMBHC up to the critical concentration. The increase in phase angle with increase in the TMBHC concentration may be attributed to the decrease in the capacitive behaviour at the metal surface due to decreased metal dissolution rate.

3.4. Effect of temperature

The effect of temperature on the corrosion rate of mild steel in 1 M hydrochloric acid and inhibition efficiency of TMBHC is studied at different temperatures in the range 30–60 °C using Tafel polarization technique. The corrosion rate increased with

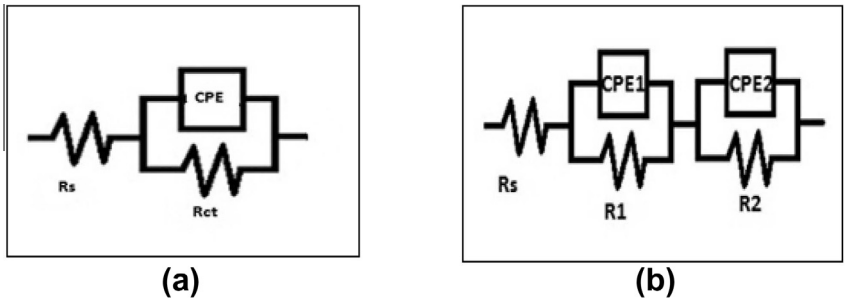

Figure 6 Equivalent circuits used to fit experimental EIS data for the corrosion of the mild steel specimen in 1 M HCl medium in the absence and presence of TMBHC.

Table 2 Impedance parameters for the corrosion of mild steel in 1 M HCl in the absence and presence of various concentrations of TMBHC.

Temp. (°C)	Conc. of inhibitor (mM)	R_1 (Ω cm^2)	R_2 (Ω cm^2)	R_p/R_{ct} (Ω cm^2)	C_{dl} (μF cm^{-2})	% *IE*
30	0			15.70	1785	–
	0.1	39.87	21.76	61.63	134.0	74.6
	0.2	51.71	27.64	79.35	100.0	80.3
	0.4	52.88	28.30	81.21	59.16	81.0
	0.6	86.00	30.40	112.0	50.48	86.1
	0.8	96.70	32.53	129.3	39.31	87.9
40	0			9.630	3761	–
	0.1	32.38	18.80	51.18	309.43	81.2
	0.2	34.00	22.00	56.00	285.06	85.3
	0.4	56.60	22.60	79.90	202.18	87.9
	0.6	72.00	23.50	95.50	133.02	90.0
	0.8	89.07	26.20	115.2	108.61	91.6
50	0			5.700	12,936	–
	0.1	31.74	17.98	49.70	683.81	88.5
	0.2	37.20	18.80	56.00	616.76	89.8
	0.4	50.50	19.63	70.19	398.42	91.8
	0.6	55.70	20.70	76.47	320.33	92.5
	0.8	59.42	23.30	82.72	256.86	93.1
60	0			1.900	55,870	–
	0.1	20.70	2.80	23.50	2642.9	91.9
	0.2	22.44	3.72	26.12	1166.1	92.7
	0.4	26.02	4.23	30.25	993.51	93.7
	0.6	26.75	5.65	32.40	736.57	94.1
	0.8	27.52	6.10	33.62	629.69	94.3

increase in temperature in the absence of inhibitor and the addition of inhibitor brought down the corrosion rate to the minimum level. Further the inhibition efficiency increased with increase in inhibitor concentration at all temperatures studied. These results facilitate the calculation of kinetic and thermodynamic parameters for the inhibition and interpret the type of adsorption followed by the inhibitor. The energy of activation is calculated using the Arrhenius equation (Yahalom, 1972).

$$\ln(CR) = B - \frac{E_a}{RT} \tag{7}$$

where B is the Arrhenius pre-exponential constant, and R is the universal gas constant. The slope $(-E_a/R)$ obtained from the Arrhenius plot (Fig. 8) of ln (CR) against $1/T$ is used to calculate the activation energy for the corrosion process. The calculated E_a values are presented in Table 3.

The energy of activation, E_a decreased with increase in inhibitor concentration due to the gradual adsorption of inhibitor molecules on mild steel, with a resultant closer approach to equilibrium during the experiment at higher temperatures (Ameer et al., 2002; Osman et al., 2003). The enthalpy and entropy of activation for the metal dissolution process are determined using the transition state Eq. (8) (Abdel Rehim et al., 1999).

$$CR = \frac{RT}{Nh}\exp\left(\frac{\Delta S^{\#}}{R}\right)\exp\left(\frac{-\Delta H^{\#}}{RT}\right) \tag{8}$$

where h is Plank's constant and N is Avogadro's number. A plot of ln (CR/T) versus $1/T$ gave a straight line (Fig. 9) with slope $= -\frac{\Delta H^{\#}}{T}$ and intercept $= \ln(R/Nh) + \frac{\Delta S^{\#}}{R}$. The positive signs of change in enthalpy $(\Delta H^{\neq})$ reflected the endothermic nature of the mild steel dissolution process (Bouklah et al., 2006). The large negative values of entropy of activation $(\Delta s^{\#})$ in the absence and presence of inhibitor imply that the activated complex in the rate determining step represents an

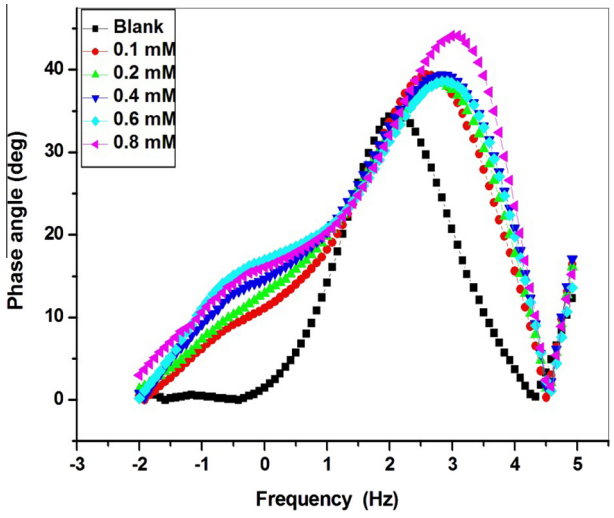

Figure 7 Bode plots for the corrosion of the mild steel specimen in 1 M HCl acid containing different concentrations of TMBHC at 40 °C.

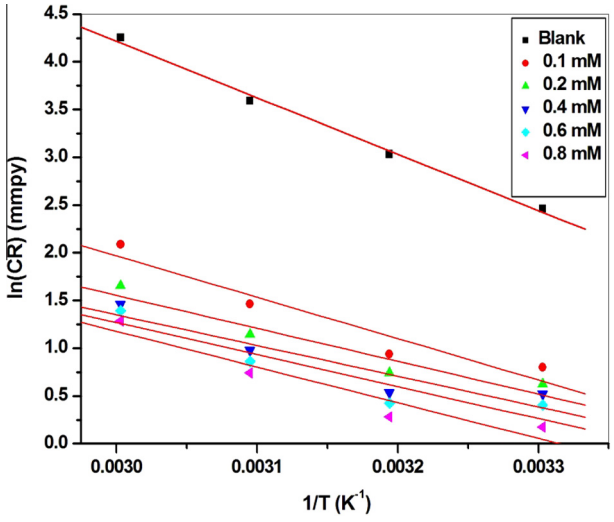

Figure 8 Arrhenius plots of ln (CR) versus $1/T$ for mild steel in 1 M HCl with different concentrations of TMBHC.

association rather than dissociation, resulting in a decrease in the randomness on going from the reactants to the activated complex (Soltani et al., 2010).

3.5. Adsorption isotherm

Tafel polarization technique is employed to find out the values of surface coverage θ at different inhibitor concentrations to understand the mechanism of corrosion inhibition and the adsorption behaviour of the inhibitor molecule on the mild steel surface. These values are used to explain the best fit isotherm to determine the adsorption process. Data are tested graphically by fitting to various isotherms. In the temperature range studied, the best correlation between the experimental results and the isotherm function is obtained using Langmuir's adsorption isotherm. Langmuir's adsorption isotherm for

Table 3 Activation parameters for the corrosion of mild steel in 1 M HCl acid containing different concentrations of TMBHC.

Conc. of inhibitor (mM)	E_a (kJ mol^{-1})	$\Delta H^{\neq}$ (kJ mol^{-1})	$\Delta S^{\neq}$ (J mol^{-1} K^{-1})
0	49.22	46.83	−71.0
0.1	36.07	33.43	−129.0
0.2	31.97	28.50	−150.4
0.4	28.72	26.08	−154.6
0.6	27.89	25.24	−159.5
0.8	26.75	24.11	−162.2

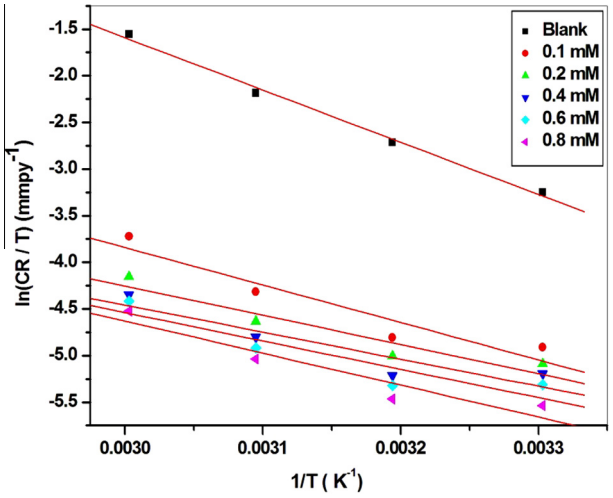

Figure 9 Plot of ln (CR)/T versus $1/T$ for the mild steel specimen in 1 M HCl containing various concentrations of TMBHC.

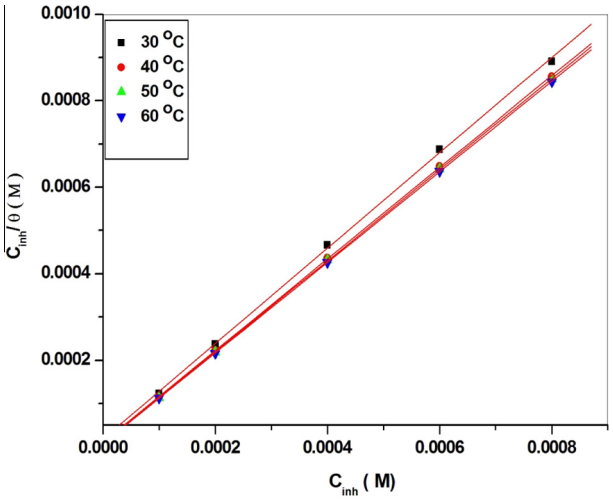

Figure 10 Langmuir's adsorption isotherm of TMBHC on mild steel in 1 M HCl at different temperatures.

monolayer chemisorption is given by the Eq. (9) (Ashassi-Sorkhabi et al., 2004).

$$\frac{C_{inh}}{\theta} = \frac{1}{K} + C_{inh} \tag{9}$$

Table 4 Thermodynamic parameters for the adsorption of TMBHC on the mild steel surface in 1 M HCl acid at different temperatures.

Temp.(°C)	$\Delta G°_{ads}$ (kJ mol^{-1})	Slope	$\Delta H°_{ads}$ (kJ mol^{-1})	$\Delta S°_{ads}$ (J mol^{-1} K^{-1})
30	−37.50	1.010		
40	−40.23	1.059	22.8	
50	−41.92	1.052		−200.2
60	−43.61	1.045		

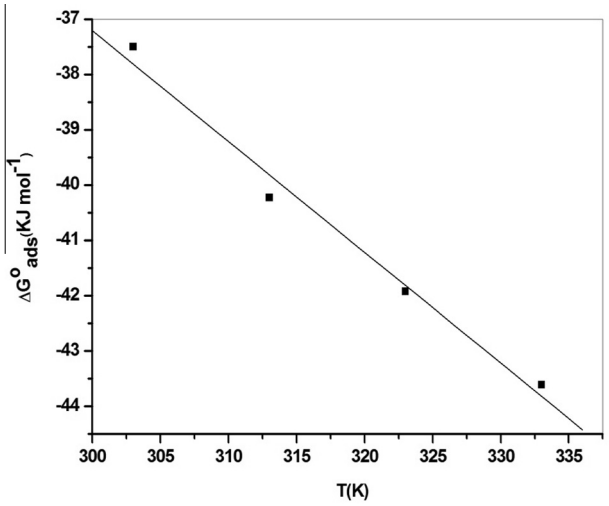

Figure 11 Plot of $\Delta G°_{ads}$ versus T for the adsorption of TMBHC on mild steel in 1 M HCl acid.

where K represents the equilibrium constant for metal-inhibitor interaction, C_{inh} is the inhibitor concentration, and θ is the degree of surface coverage. The plot of C_{inh}/θ versus C_{inh} gave a straight line as shown in Fig. 10 and the intercept values were used to calculate the equilibrium constant K. Further the standard free energy change $\Delta G°_{ads}$ values for the adsorption are calculated using Eq. (10) (Olivares et al., 2006).

$$K = \frac{1}{55.5}\exp\frac{-\Delta G^{\circ}_{ads}}{RT} \quad (10)$$

where K is the equilibrium constant, R is the universal gas constant and T is the absolute temperature and 55.5 is the concentration of water in solution in mol/dm^3. The negative values of $\Delta G°_{ads}$ ensured the spontaneity of the adsorption process and stability of the adsorbed layer on the mild steel surface (Ahamad et al., 2010). Generally, the values of $\Delta G°_{ads}$ around −20 kJ mol^{-1} or more positive are consistent with physisorption, while those around −40 kJ mol^{-1} or more negative with chemisorption (Quraishi et al., 2000). The value of $\Delta G°_{ads}$ for the studied inhibitor is given in Table 4. The absolute value of $\Delta G°_{ads}$ increased with increase in temperature which indicates that the adsorption became favourable with increasing temperatures and also the inhibitor molecules are chemically adsorbed on the mild steel surface (Noor and Al-Moubaraki, 2008). The enthalpy and entropy for the adsorption of TMBHC on mild steel are deduced by using the thermodynamic Eq. (11) (Bouklah et al., 2006).

$$\Delta G^{\circ}_{ads} = \Delta H^{\circ}_{ads} - T\Delta S^{\circ}_{ads} \quad (11)$$

Fig. 11 represents the plot of $\Delta G°_{ads}$ versus T. The corresponding standard enthalpy of adsorption $\Delta H°_{ads}$ and the standard entropy of adsorption ($\Delta S°_{ads}$) are computed from the slope and intercept of the straight line respectively. The thermodynamic parameters are tabulated in Table 4.

The positive sign of $\Delta H°_{ads}$ in 1 M HCl solution indicated that the adsorption of inhibitor molecule is an endothermic process. In general, an endothermic process is attributed to chemisorption while an exothermic adsorption process signifies either physisorption or chemisorption (Durnie et al., 2001). In the present study, the calculated value of $\Delta H°_{ads}$ with positive sign (22.8 kJ mol^{-1}) indicates the chemisorption of inhibitor. The $\Delta S°_{ads}$ value is large and negative, indicating that the decrease in disordering takes place on going from the reactant to the adsorbed species (Martinez and Stern, 2002).

3.6. Inhibition mechanism

Corrosion inhibition of many metals in acidic solution can be described based on adsorption phenomenon. In the present study the adsorption of TMBHC on the mild steel specimen can be attributed to either sharing of electrons between the hetero atoms and iron or π electron interactions between the aromatic ring of the TMBHC and the metal surface (Khaled and Hackerman, 2003). Adsorption can also occur

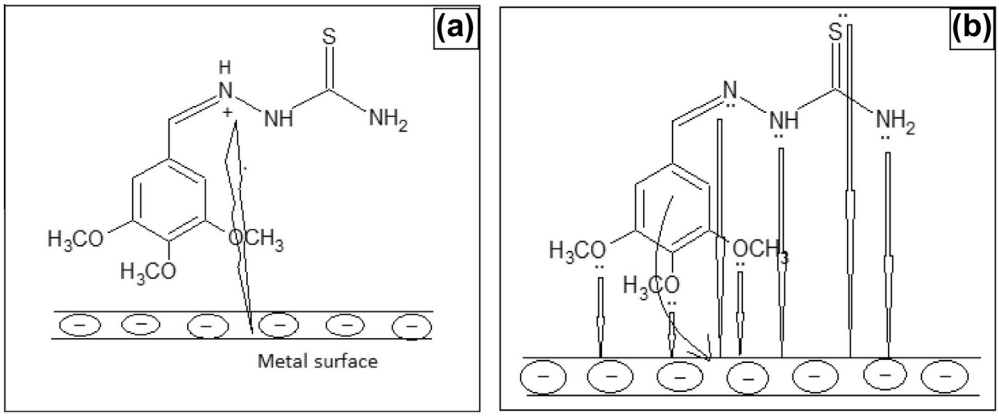

Figure 12 Skeletal representation of the mode of adsorption of TMBHC on the metal surface.

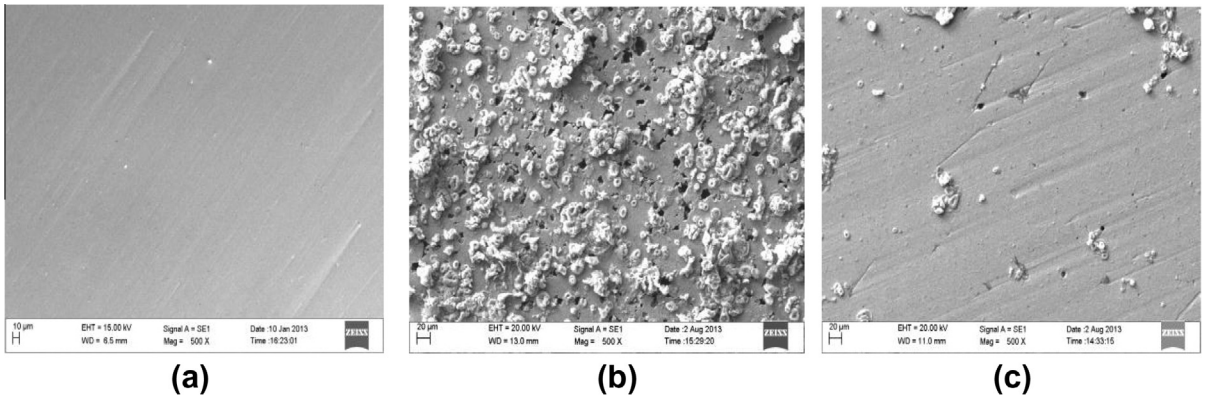

Figure 13 SEM images of mild steel (a) freshly polished specimen surface, (b) exposed to 1 M HCl solution and (c) exposed to 1 M HCl containing 0.8 mM of TMBHC.

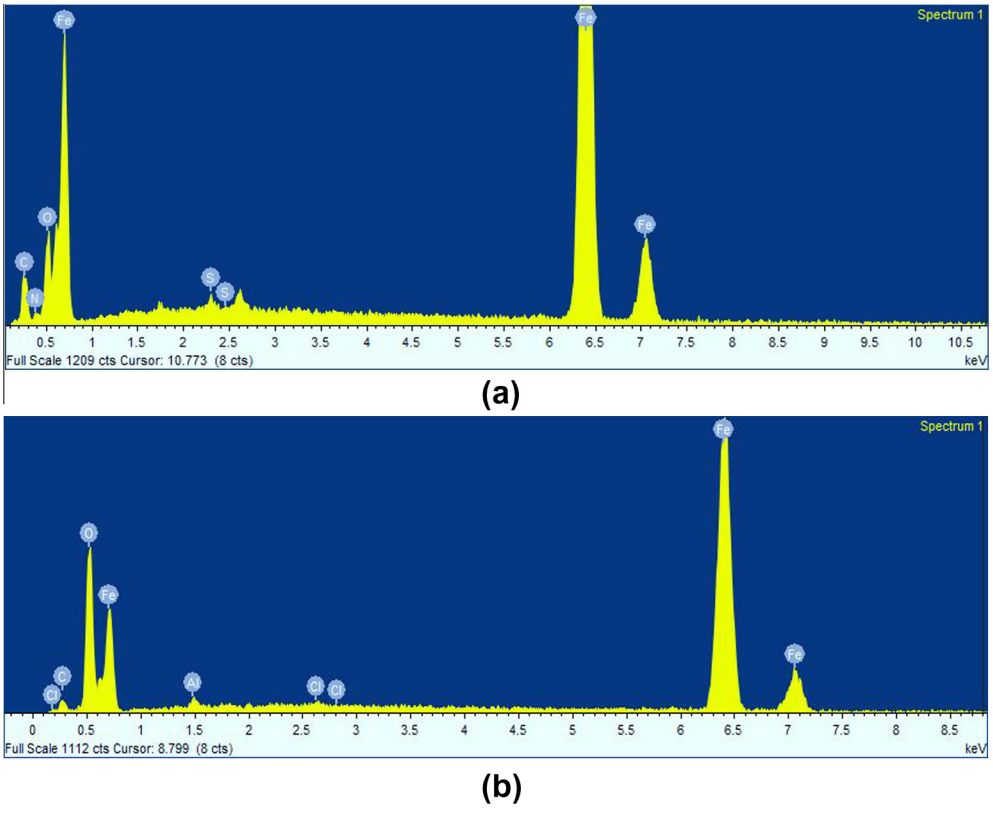

Figure 14 EDX spectrum of mild steel (a) exposed to 1 M HCl, (b) exposed to1 M HCl containing 0.8 mM of TMBHC.

via electrostatic interaction between a negatively charged metal surface and the positive charge of the inhibitor molecule or by charge sharing or charge transfer from the inhibitor molecules to the metal surface to form a coordinate type of bond.

In the present case TMBHC molecules get protonated in HCl medium at nitrogen atoms, which results in the formation of positively charged inhibitor species. When mild steel is immersed in HCl solution in the presence of inhibitor, chloride ions are initially adsorbed onto the metal surface (a), because of smaller degree of hydration. The adsorbed chloride ions generate an excess of negative charge towards the solution by forming negatively charged metal surface which favour more adsorption of the positively charged inhibitor molecule (b). The protonated TMBHC molecules are now adsorbed on metal surface by replacing the Cl^- (c) ions, there by facilitating physisorption (Khaled and Hackerman, 2003). In addition, the protonated inhibitor molecules can also be adsorbed at cathodic sites of metal in competition with the hydrogen ions. The adsorption of protonated TMBHC molecules reduces the rate of hydrogen evolution reaction along with metal oxidation resulting in physisorption. The possible inhibition mechanism and its path way in the presence of TMBHC in HCl medium is represented below.

$$Fe + Cl^- \leftrightarrow \underset{(a)}{(FeCl^-)_{ads} + Inh^+} \leftrightarrow \underset{(b)}{(FeCl^-\ Inh^+)_{ads}} \leftrightarrow \underset{(c)}{(Fe\ Inh^+)_{ads} + Cl^-}$$

Further the unprotonated or neutral molecule of TMBHC can also adsorb via chemisorption on the vacant sites on the mild steel surface either by, sharing of electrons between the hetero atoms of TMBHC and the metal surface or by the interaction of π electrons of the aromatic ring of the TMBHC molecule with that of the mild steel surface. The vacant 3d orbital of iron can form coordinate type of bond with inhibitor due to the interaction of π-electron clouds of aromatic rings as well as unshared electron pairs on nitrogen or oxygen atoms of the TMBHC leading to predominant chemisorption (Popova et al., 2003).

The possible adsorption of TMBHC on the mild steel surface through electrostatic interaction and e-pair interaction is shown in Fig. 12(a) and (b), respectively.

3.7. Scanning electron microscopy (SEM) and Energy-dispersive X-ray spectroscopy (EDS) analysis

SEM investigations were carried out to differentiate between the surface morphology of the metal surface after its immersion in 1 M hydrochloric acid in the absence and presence of TMBHC for about two hours. Fig. 13(a) shows the freshly polished mild steel surface. Fig. 13(b) shows the facets due to the corrosive action of 1 M hydrochloric acid on the mild steel surface with cracks and rough surface. Smooth sample surface without any visible corrosion attack or pits in the presence of TMBHC is shown in Fig. 13(c). This confirms the adsorption of TMBHC on the mild steel surface through the formation of protective film.

EDS investigations were carried out in order to identify the composition of the species formed on the metal surface in 1 M Hydrochloric acid in the absence and presence of TMBHC. The corresponding EDS profile analyses for the selected areas on the SEM images of Fig. 13(b) and (c) are shown in Fig. 14(a) and (b), respectively. The atomic percentage of the elements found in the EDS profile for the corroded metal surface is 45.29% O, 1.01% Cl and 38.92% Fe. This indicates that the corrosion of mild steel is due to the formation of iron oxide on the metal surface. Similarly, elemental composition obtained in the presence of TMBHC (16.22% O, 3.4% N, 0.41% S and 45.86% Fe) proves the formation of inhibitor film in this area.

4. Conclusion

Based on the results of investigation, the following conclusions are drawn:

(1) TMBHC acts as a potential inhibitor by controlling both hydrogen evolution and metal dissolution, there by acting as a mixed type of inhibitor.
(2) Inhibition efficiency increases with increasing TMBHC concentration and also with increasing temperature.
(3) Adsorption isotherm of TMBHC on the metal surface follows Langmuir's adsorption isotherm.
(4) Evaluation of activation and thermodynamic parameters shows mixed adsorption with predominantly chemical adsorption of TMBHC on the metal surface.
(5) Inhibition action of TMBHC takes place through its adsorption on the metal surface, which is confirmed by surface morphology study.

References

Abdel Rehim, S.S., Magdy, A.M., Ibrahim, K.F., 1999. 4-Aminoantipyrine as an inhibitor of mild steel corrosion in HCl solution. J. Appl. Electrochem. 29, 593–599.
Ahamad, I., Prasad, R., Quraishi, M.A., 2010. Thermodynamic, electrochemical and quantum chemical investigation of some Schiff bases as corrosion inhibitors for mild steel in hydrochloric acid solutions. Corros. Sci. 52, 933–942.
Ameer, M.A., Khamis, E., Al-Senani, G., 2002. Effect of temperature on stability of adsorbed inhibitors on steel in phosphoric acid solution. J. Appl. Electrochem. 32, 149–156.
Amin, M.A., Abd El-Rehim, S.S., El-Sherbini, E.E.F., Bayyomi, R.S., 2007. The inhibition of low carbon steel corrosion in hydrochloric acid solutions by succinic acid: part I. Weight loss, polarization, EIS, PZC, EDX and SEM studies. Electrochim. Acta 52, 3588–3600.
Ashassi-Sorkhabi, H., Majidi, M.R., Seyyedi, K., 2004. Investigation of inhibition effect of some amino acids against steel corrosion in HCl solution. Appl. Surf. Sci. 225, 176–185.
Badr, G.E., 2009. The role of some thiosemicarbazide derivatives as corrosion inhibitors for C-steel in acid medium. Corros. Sci. 51, 2529–2536.
Bentiss, F., Traisnel, M., Lagrenee, M., 2001. Influence of 2,5-bis (4-imethylaminophenyl)-1,3,4-thiadiazole on corrosion inhibition of mild steel in acidic media. J. Appl. Electrochem. 31, 41–48.
Bouklah, M., Hammouti, B., Lagrenee, M., Bentiss, F., 2006. Thermodynamic properties of 2,5-bis(4-methoxyphenyl)-1,3,4-oxadiazole as corrosion inhibitor for mild steel in normal sulfuric acid medium. Corros. Sci. 48, 2831–2842.
Durnie, DeMarco, R., Kinsella, B., Jefferson, A., 2001. A study of adsorption properties of commercial carbon dioxide corrosion inhibitor formulations. J. Electrochem. Soc. 31, 1221–1226.
El Kadher, A., ElWarraky, J.M., Abd el Aziz, A.M., 1998. Corrosion inhibition of mild steel by sodium tungstate in neutral solution part 1: behaviour in distilled water. Br. Corros. J. 33, 139–144.
Emregul, K.C., Hayval, M., 2006. Studies on the effect of a newly synthesized Schiff base compound from phenazone and vanillin on the corrosion of steel in 2 M HCl. Corros. Sci. 48, 797–812.
Fekry, A.M., Riham, R.M., 2010. Acetyl thiourea chitosan as an eco-friendly inhibitor for mild steel in sulphuric acid medium. Electrochim. Acta 55, 1933–1939.
Hegazy, M.A., Ahmed, H.M., El-Tabei, A.S., 2011. Investigation of the inhibitive effect of p-substituted 4-(N,N, N-dimethyldodecylammonium bromide)benzylidene-benzene-2-yl-amine on corrosion of carbon steel pipelines in acidic medium. Corros. Sci. 53, 671–678.
Hosseini, M., Mertens, S.F.L., Ghorbani, M., Arshadi, M.R., 2003. Asymmetrical Schiff bases as inhibitors of mild steel corrosion in sulphuric acid media. Mater. Chem. Phys. 78, 800–808.
Hudson, R.M., Warning, C.J., 1970. Influence of halide mixtures with organic compounds on dissolution and hydrogen absorption by low C-steel in H_2SO_4. Corros. Sci. 10, 121–134.
Khaled, K.F., Hackerman, N., 2003. Investigation of the inhibitive effect of *ortho*-substituted anilines on corrosion of iron in 1 M HCl solutions. Electrochem. Acta 48, 2715–2723.
Legrenee, M., Mernari, B., Bouanis, M., Traisnel, M., Bentiss, F., 2002. Study of the mechanism and inhibiting efficiency of 3,5-bis (4-

Please cite this article in press as: Preethi Kumari, P. et al., Electrochemical measurements for the corrosion inhibition of mild steel in 1 M hydrochloric acid by using an aromatic hydrazide derivative. Arabian Journal of Chemistry (2014), http://dx.doi.org/10.1016/j.arabjc.2014.09.005

methylthiophenyl)-4H-1,2,4-triazole on mild steel corrosion in acidic media. Corros. Sci. 44, 573–588.
Li, W.H., He, Q., Pei, C.L., Hou, B.R., 2007. Experimental and theoretical investigation of the adsorption behavior of new triazole derivatives as inhibitors for mild steel corrosion in acid media. Electrochim. Acta 52, 6386–6397.
Li, W., He, Q., Zhang, S., Pei, C., Hou, B., 2008. Some new triazole derivatives as inhibitors for mild steel corrosion in acidic medium. J. Appl. Electrochem. 38, 289–295.
Lowmunkhong, P., Ungthararak, D., Sutthivaiyakit, P., 2010. Tryptamine as a corrosion inhibitor of mild steel in hydrochloric acid solution. Corros. Sci. 52, 30–36.
Machnikova, E., Kenton, W.H., Hackerman, N., 2008. Corrosion inhibition of carbon steel in hydrochloric acid by furan derivatives. Electrochim. Acta 53, 6024–6032.
Martinez, S., Stern, I., 2002. Thermodynamic characterization of metal dissolution and inhibitor adsorption processes in the low carbon steel/mimosa tannin/sulfuric acid system. Appl. Surf. Sci. 199, 83–89.
Nada, F.A., Fekry, A.M., Hamdi, M.H., 2011. Corrosion inhibition, hydrogen evolution and antibacterial properties of newly synthesized organic inhibitors on 316L stainless steel alloy in acid medium. Int. J. Hydrogen Energy 36, 6462–6471.
Noor, E.A., Al-Moubaraki, A.H., 2008. Thermodynamic study of metal corrosion and inhibitor adsorption processes in mild steel/1-methyl-4[4′(-X)-styryl pyridinium iodides/hydrochloric acid systems. Mater. Chem. Phys. 110, 145–154.
Olivares, O., Likhanova, N.V., Gomez, B., Navarrete, J., Llanos-Serrano, M.E., Arce, E., Hallen, J.M., 2006. Electrochemical and XPS studies of decylamides of a-aminoacids adsorption on carbon steel in acidic environment. Appl. Surf. Sci. 252, 2894–2909.
Osman, M.M., El-Ghazawy, R.A., Al-Sabagh, A.M., 2003. Corrosion inhibitor of some surfactants derived from maleic–oleic acid adducts on mild steel in 1 M H_2SO_4. Mater. Chem. Phys. 80, 55–62.
Popova, A., Sokolova, E., Raicheva, S., Christov, M., 2003. AC and DC study of the temperature effect on mild steel corrosion in acid media in the presence of benzimidazole derivatives. Corros. Sci. 45, 33–58.
Quraishi, M.A., Rawat, J., Ajmal, M., 2000. Dithiobiurets: a novel class of acid corrosion inhibitors for mild steel. Appl. Electrochem. 30, 745–751.
Quraishi, M.A., Sardar, R., Jamal, D., 2001. Corrosion inhibition of mild steel in hydrochloric acid by some aromatic hydrazides. Mater. Chem. Phys. 71, 309–313.
Raistrick, I.D., Franceschetti, D.R., Macdonald, J.R., Barsoukov, E., Macdonald, J.R. (Eds.), 2005. Impedance Spectroscopy, second ed., Theory, Experimental, and Applications. John Wiley & Sons, New Jersey.
Renata, B.O., Elaine, M.S.F., Rodrigo, P.P.S., Anderson, A.A., Antoniana, U.K., Carlos, L.Z., 2008. Synthesis and antimalarial activity of semicarbazone and thiosemicarbazone derivatives. Eur. J. Med. Chem. 43, 1983–1988.
Shahin, M., Bilgic, S., Yilmaz, H., 2003. The inhibition effects of some cyclic nitrogen compounds on the corrosion of the steel in NaCl medium. Appl. Surf. Sci. 195, 1–7.
Shanbhag, A.V., Venkatesha, T.V., Prabhu, R., Kalkhambkar, R.G., Kulkarni, G.M., 2008. Corrosion inhibition of mild steel in acidic medium using hydrazide derivatives. J. Appl. Electrochem. 38, 279–287.
Singh, A.K., 2012. Inhibition of mild steel corrosion in hydrochloric acid solution by 3-(4-((Z)-Indolin-3-ylideneamino) phenylimino)indolin-2-one. Ind. Eng. Chem. Res. 51, 3215–3223.
Singh, A.K., Quraishi, M.A., 2010. Effect of cefazolin on the corrosion of mild steel in HCl solution. Corros. Sci. 52, 152–160.
Singh, A.K., Quraishi, M.A., 2012. Study of some bidentate schiff bases of isatin as corrosion inhibitors for mild steel in hydrochloric acid solution. Int. J. Electrochem. Sci. 7, 3222–3241.
Singh, D.D.N., Singh, T.B., Gaur, B., 1995. The role of metal cations in improving the inhibitive performance of hexamine on the corrosion of steel in hydrochloric acid solution. Corros. Sci. 37, 1005–1019.
Soltani, N., Behpour, M., Ghoreishi, S.M., Naeimi, H., 2010. Corrosion inhibition of mild steel in hydrochloric acid solution by double Schiff bases. Corros. Sci. 52, 1351–1361.
Tao, Z., Zhang, S., Li, W., Hou, B., 2009. The role of metal cations in improving the inhibitive performance of hexamine on the corrosion of steel in hydrochloric acid solution. Corros. Sci. 51, 2588–2595.
Wang, X., Yang, H., Wang, F., 2010. A cationic gemini-surfactant as effective inhibitor for mild steel in HCl solutions. Corros. Sci. 52, 1268–1276.
Wei-hua, L., Qiao, H., Sheng-tao, Z., Chang-ling, P., Hou, B., 2008. Some new triazole derivatives as inhibitors for mild steel corrosion in acidic medium. J. Appl. Electrochem. 38, 289–295.
Yahalom, J., 1972. The significance of the energy of activation for the dissolution reaction of metal in acids. Corros. Sci. 12, 867–868.
Zhao, M., Liu, M., Ling Song, G., Atrens, A., 2008. Influence of pH and chloride ion concentration on the corrosion of Mg alloy ZE41. Corros. Sci. 50, 3168–3178.

Please cite this article in press as: Preethi Kumari, P. et al., Electrochemical measurements for the corrosion inhibition of mild steel in 1 M hydrochloric acid by using an aromatic hydrazide derivative. Arabian Journal of Chemistry (2014), http://dx.doi.org/10.1016/j.arabjc.2014.09.005